Revelation and Science
Vol. 13, No. 02 (1445H/2023) 52-61

Nonlinear Rotations on a 3-Dimensional Lattice

Mohammad Hanif Saleh, Wan Nur Fairuz Alwani Wan Rozali, Siti Fatimah Zakaria
Dynamical Systems and Their Applications (DSTA) Research Unit, Department of Computational and Theoretical Sciences, Kulliyyah of Science,
International Islamic University Malaysia, 25200 Kuantan, Pahang, Malaysia

Abstract
The study of resonances of Hamiltonian systems with a divided phase space is a well-established area of research which attracted the interests of many researchers over the years. We study such resonances over a discrete space focusing on the rotational motion of some orbits in the 3-Dimensional lattice, $\mathbb{Z}^3$. In this study, we construct the discrete standard map from 2-Dimensional to 3-Dimensional lattices. Then, we identify and categorize any transformation that could give periodicity for the 3-Dimensional lattice on a specific map. The study aims to determine the points that give the periodicity and at the same time investigate the behavior of the points for the nonlinear stable orbits over a discrete space. For some choice of parameters α and β, our findings showed that the orbit of the 3-Dimensional map is periodic depending on the initial conditions. Some arbitrary initial conditions may be periodic in a 3-Dimensional lattice.
Keywords: Hamiltonian systems, nonlinear rotations, space discretization, arithmetic dynamics.

Abstrak
Kajian resonans sistem Hamiltonian dengan ruang fasa terbahagi adalah bidang penyelidikan yang dikenali menarik minat ramai penyelidik bertahun-tahun. Kami mengkaji resonans ini di atas ruang diskret yang memfokuskan pada gerakan putaran beberapa orbit dalam kekisi 3 Dimensi, Z^3. Dalam kajian ini, kami membina peta piawai diskret daripada kekisi 2 Dimensi kepada 3 Dimensi. Kemudian, kami mengenal pasti dan mengkategorikan sebarang transformasi yang boleh memberikan keberkalaan untuk kekisi 3 Dimensi pada peta tertentu. Kajian ini bertujuan untuk menentukan titik-titik yang memberikan keberkalaan dan pada masa yang sama menyiasat kelakuan titik-titik untuk orbit stabil tak linear di atas ruang diskret. Untuk beberapa pilihan parameter, penemuan kami menunjukkan bahawa orbit peta 3 Dimensi adalah berkala bergantung pada keadaan awal. Sesetengah keadaan awal mungkin berkala dalam kekisi 3 Dimensi.
Kata kunci: Sistem Hamiltonian, putaran tak linear, pendiskretan ruang, dinamik aritmetik.

**Corresponding author:*
Wan Nur Fairuz Alwani Binti Wan Rozali
Kulliyyah of Science,
International Islamic University Malaysia
Email: fairuz_wnfawr@iium.edu.my

Introduction

The study of Chirikov-Taylor standard map on a divided phase space has been studied for many years (Chirikov, 1969; 1979; 1983; Chirikov, Izrailev, & Shepelyansky, 1981; Chirikov & Shepelyansky, 1984). The map is obtained from a problem of physical system such as kicked rotor which can be defined on a cylinder phase space $\mathbb{T} = \mathbb{R}/\mathbb{Z}$ as follows:

$$\begin{aligned} &S: \mathbb{T}^2 \to: \mathbb{T}^2, \\ &p_{n+1} = p_n + k \sin q_n, \\ &q_{n+1} = q_n + p_{n+1}, \end{aligned} \tag{1}$$

where k is the perturbation parameter, p_n is the momentum and q_n is the angle produced from the kicked rotor. One can study the map in equation (1) in a discrete space.

The process for space discretization can be done in many ways (Vivaldi & Bailin, 2015). One of the methods of space discretization is to replace the torus $\mathbb{T}^2$ by an $N \times N$ lattice. However, replacing the torus with a lattice can create problems. This is due to the torus having points which may not exactly “sit” on the discrete point on a lattice. Thus, space discretization could be done with the conditions that the map preserves the lattice and is invertible (Rannou, 1974).

Following Rannou's pioneering work, discretization has been used for a variety of purposes including simulating quantum effects in classical systems, achieving invertibility in a delicate numerical experiment, arithmetically characterizing Hamiltonian chaos, and investigating various phenomena related to numerical orbits.

For a discrete version of the Chirikov-Taylor standard map in equation (1), the map is defined on a doubly periodic square lattice $(\mathbb{Z}/N\mathbb{Z})^2$ as follows:

$$\begin{aligned} &\gamma: (\mathbb{Z}/N\mathbb{Z})^2 \to (\mathbb{Z}/N\mathbb{Z})^2, \\ &\begin{cases} y_{t+1} \equiv y_t + V(x_t) \ \ (mod\ N) \\ x_{y+1} \equiv x_t + y_{t+1} \ \ (mod\ N) \end{cases}, \end{aligned} \tag{2}$$

$$V(x) = \begin{cases} +1, \ 0 \le x < \left\lfloor \frac{N}{2} \right\rfloor \\ -1, \ \left\lfloor \frac{N}{2} \right\rfloor \le x < N \end{cases}, \tag{3}$$

where V is the perturbation function of the discrete map and N is a large, fixed integer. The equation in equation (2) has been constructed by Zhang and Vivaldi (1998). The discrete version of the map in equation (2) is plotted and can be shown in Figure 1(b) below.

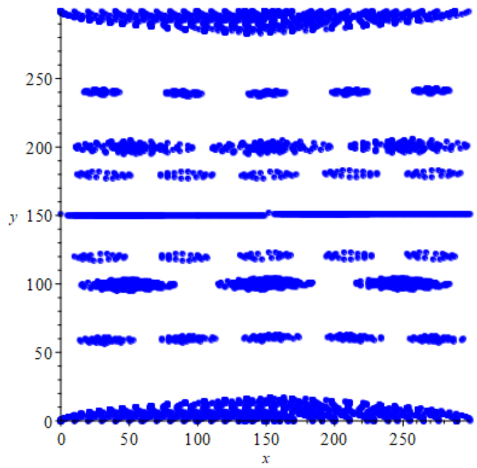

(a)

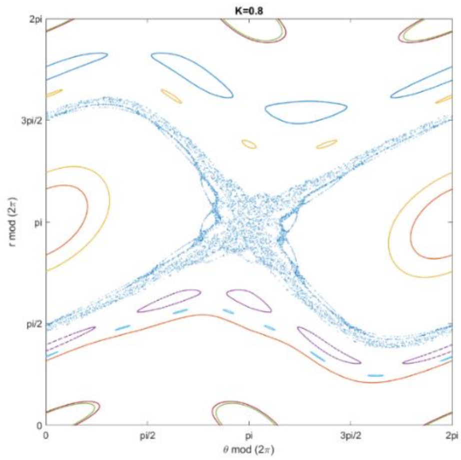

(b)

Figure 1: The island chains for a) Poincare sections of the standard map on a torus when $k = 0.8$, b) The discrete orbits of the map in equation (2) with $N = 300$, and $V(x)$ given by equation (3).

In Figure 1(a), there exists Kolmogorov-Arnold-Moser curves (or invariant curves) which bound the motions of the orbit points (Finn, 2008; Jürgen, 2001). As the perturbation k increases (sufficiently small), more and more island chains of higher order exist. Meanwhile, the discrete version in Figure 1(b) features a discrete version of dynamics on a divided phase space. Some islands filled with periodic points are formed and have island chains of odd order. Further, there is no existence of invariant curves to bound the discrete orbits. Thus, in one of the islands of the map in equation (2), we defined a local mapping where the periodic orbits are bounded. We are looking for cases where the local dynamics can allow bounded invariant sets because the latter can be realized in the global mapping by selecting N large enough.

The local mapping in one of the islands has been constructed by Zhang and Vivaldi on 2-dimensional lattice $\mathbb{Z}^2$ which is defined by,

$$\emptyset: \mathbb{Z}^2 \to \mathbb{Z}^2,$$
$$Y_{n+1} = Y_n - sign(X_n),$$
$$X_{n+1} = X_n + \alpha Y_{n+1} + \beta,$$
$$\alpha \geq 1, \quad 0 \leq \beta < \alpha,$$
where
$$sign(X) = \begin{cases} +1, if\ X \geq 0 \\ -1, if\ X < 0 \end{cases}. \qquad (4)$$

Here, α and β are non-negative integers. In this map, the parameter α represents the "stretching" of the elliptic-type orbits in horizontal direction and the parameter β can be viewed as the "shrinking" of the elliptic-type orbits in the vertical direction. The behavior of the discrete points $\emptyset$ defined in equation (4) is discussed in detail in the paper by Alwani and Vivaldi (2018). They have proved that if $\bar{\alpha} = \frac{\alpha}{gcd(\alpha,2\beta)}$, then the period of the orbit $\emptyset$ does not exceed $\bar{\alpha}$. Moreover, for sufficiently large values of initial conditions, all orbits have period $\bar{\alpha}$. In other words, the orbits of the map $\emptyset$ closes its rotation around the origin (see Figure 2(a)). They also have proved for the non-periodic case that is, if $\bar{\alpha}$ is even (or α divisible by 4), then all orbits will eventually reach infinity and escape in both time directions. In this case, the orbit of $\emptyset$ never closes its rotation forever.

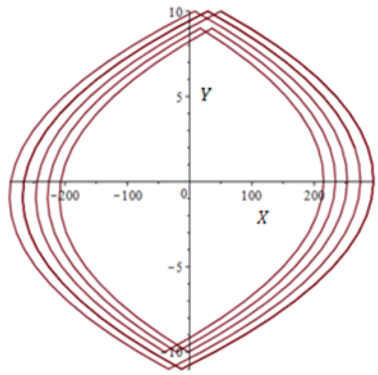

(a)

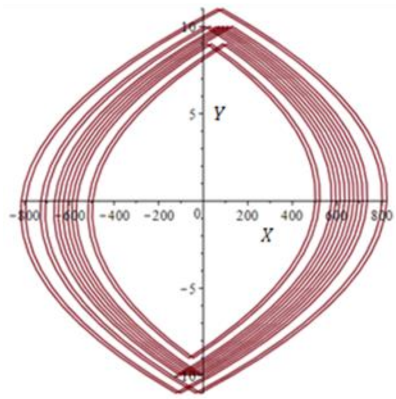

(b)

Figure 2: Elliptic-type orbits of the local mapping in equation (4); a) The orbit of $\emptyset$ for $\alpha = 5, \beta = 2$. b) The orbit of $\emptyset$ for $\alpha = 13, \beta = 2$.

In Figure 2, the orbit of $\emptyset$ defined in equation (4) intersects the non-negative X-axis $\bar{\alpha}$ times, and the orbit is periodic with period $\bar{\alpha}$. As we increase the value of X, the longer time it takes for the orbit of $\emptyset$ to complete a rotation around the origin (0,0) in this 2-D map.

This research is motivated by the question of what happens to the trajectory of this 2-dimensional (2-D) space orbits in the 3-dimensional (3-D) space? Basically, in paper (Alwani & Vivaldi, 2018), this 2-D lattice is reduced to the 1-dimensional (1-D) lattice by using Poincaré surface of section that is defined by $\Sigma = \{(X, 0) \in \mathbb{Z}^2 : X \geq 0\}$. We will modify this 2-D map defined in equation (4) by adding "extra" Z-axis in the map to investigate the orbits in the 3-D space. The extra Z-axis is applied to the 2-D map in such a way that the 2-D orbits can be viewed in 3-D space. One of the objectives is to check the periodicity orbits. Does the periodicity of the orbits can be reached in the 3-D space? Some cases will be considered in this paper.

Heinrich and Hansen (2020) presented in their paper, a highly accurate unsupervised learning method for 3-D computed tomography (CT) registration for the abdomen that employs a discrete displacement layer and a probabilistic evaluation of a contrast-invariant metric. By iteratively subdividing the 3-D search space into orthogonal planes, they achieved a significant reduction in memory and processing load. As a result, by using a fully 3-D discrete network, they were able to reach more in terms of accuracy to complete this medical part. Other related papers on 3-D space can also be found in (Hofmann et al., 2017; Samaniego, Sanchis, García-Nieto & Simarro, 2017; Thibault, 2010). Some of the methodology discussed in the results and discussion may be referred to (Dawkins, n.d.). Other papers related to dynamical systems viewed in 3-D are also described in (Haramburu, 2006; Lucas, Sander & Taalman, 2020). In these two papers, they visualize the system of dynamics in 3-D modeling.

The study of 3-D modeling and methods have been increasingly growing in the study of technology. In (Bane, 2012), the 3-D modeling not only aims to create the models but also able to visualize the structure of the models when it takes its form. In other words, it is a test whether the structure of the 3-D models can be realistically created and ideal for its purposes. Thus, in this paper, we only focus on the dynamics of the orbits of the 2-D map which can viewed in the 3-D map.

Methodology

Construction of 3-D Map

As we mentioned in the introduction, we add the extra axis in the map defined in equation (4). There are infinitely many choices of equations that we can define for the extra "Z-axis". The simplest case for modifying the 2-D map in equation (4) into a 3-D map is by letting $Z_{n+1} = c$ where c is an integer. In this case, one can observe that the orbit of $\emptyset$ is lifted from a plane XY by an integer c.

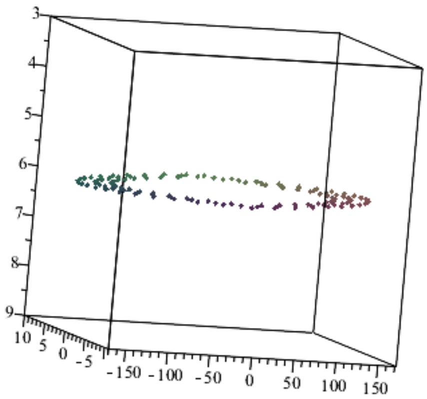

Figure 3: The elliptic-type orbits shown in Figure 2 (a) is "lifted" by an integer with $Z_{n+1} = 6$ in a 3-D space.

Since the periodic orbit of the map $\emptyset$ defined in equation (4) on the XY-plane is lifted upward by an integer 6, then it can be observed that the map $\emptyset$ is also periodic in a 3-D discrete space.

Construction of 3-D Map: Case I

Now, we are interested to study the elliptic-type orbits for some other cases of Z_{n+1}. From equation (4), we construct the map on a 3-D lattice as follows, Case I:

$$\overline{\Phi}: \mathbb{Z}^3 \rightarrow \mathbb{Z}^3,$$
$$\alpha \geq 1, \quad 0 \leq \beta < \alpha,$$
$$Y_{n+1} = Y_n - sign(X_n),$$
$$X_{n+1} = X_n + \alpha Y_{n+1} + \beta,$$
$$\overline{Z}_{n+1} = \overline{Z}_n + sign(X_n),$$

where

$$sign(X) = \begin{cases} +1, if\ X \geq 0 \\ -1, if\ X < 0 \end{cases} \qquad (5)$$

Here, α and β are non-negative integers. We denote (x_0, y_0, z_0) to define the initial conditions and (X_0, Y_0, Z_0) to define the function of X, Y and Z. In the above case in equation (5), $\overline{Z}_{n+1}$ is the equation which has been added into the map $\emptyset$ defined in equation (4). It gives the value of an integer for any initial condition (x_0, y_0, z_0) in the orbit of $\overline{\Phi}$. The $\overline{Z}_{n+1}$ in equation (5) is added in such a way that the form of the elliptic-type orbits is preserved. The equation of Z_{n+1} in Figure 3 is chosen different from the $\overline{Z}_{n+1}$ in equation (5) as the equation of $\overline{Z}_{n+1}$ depends on the initial value of (x_0, y_0, z_0) and the $sign(X_n)$. In the next section, we will discuss some numerical observations of the orbit of $\overline{\Phi}$.

Numerical Experiments on Case I

In Case I, one observes from the numerical experiments, periodicity of the orbit of $\overline{\Phi}$ defined in equation (5) can be achieved in a 3-D discrete space.

The orbit of $\overline{\Phi}$ is similar to that of orbit of $\emptyset$ defined in equation (4) except that it is the orbit that rotates around its center on the YZ-plane which is lifted by 45° angle from the horizontal plane (see Figure 4).

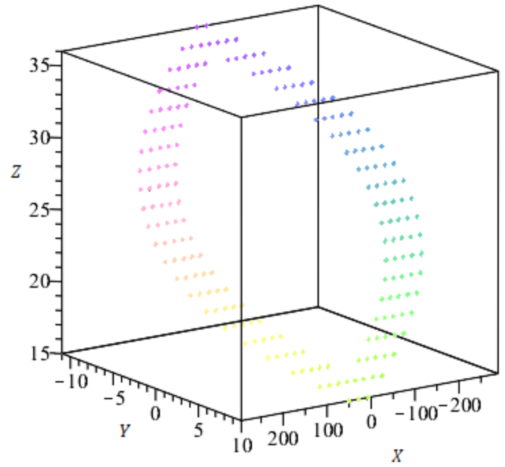

(a)

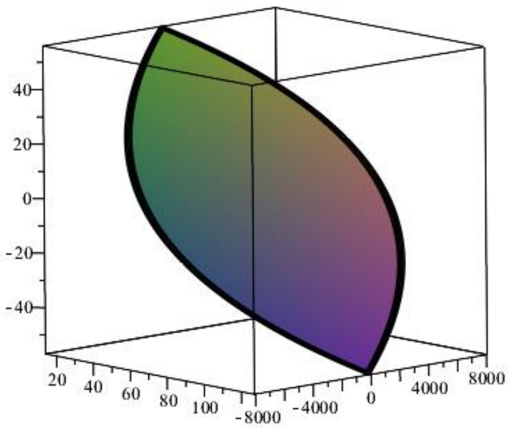

(b)

Figure 4: The orbit of $\overline{\Phi}$ defined in equation (5) with $\alpha = 5, \beta = 2$ in a 3-D lattice. a) The orbit of $\overline{\Phi}$ forms an elliptic-type orbits as in the XY plane defined in equation (4) and complete the rotations $\bar{\alpha}$ times. b) The map of $\overline{\Phi}$ plotted in a polygon plot.

It rotates around its elliptic-type center point $\bar{\alpha}$ times, which makes the orbit of Φ is periodic with period $\bar{\alpha}$. Moreover, the orbit of $\overline{\Phi}$ involves the revolution around its center point on a specific plane instead of the whole 3-D space $\mathbb{Z}^3$.

Construction of 3-D Map: Case II

Now, let us consider a different case of the 3-D. Again, from equation (4), we change the equation defined for the Z-axis in equation (4) as follows:

Case II:

$$\begin{aligned}
&\widetilde{\Phi}: \mathbb{Z}^3 \to \mathbb{Z}^3,\\
&\alpha \geq 1,\ 0 \leq \beta < \alpha,\\
&Y_{n+1} = Y_n - sign(X_n),\\
&X_{n+1} = X_n + \alpha Y_{n+1} + \beta,\\
&\tilde{Z}_{n+1} = X_n Y_n + \alpha sign(\tilde{Z}_n) - \beta -\\
&Y_{n+1} + X_{n+1},
\end{aligned} \tag{6}$$

where,

$$sign(X) = \begin{cases} +1, if\ X \geq 0 \\ -1, if\ X < 0 \end{cases},$$

and

$$sign(Z) = \begin{cases} +1, if\ Z \geq 0 \\ -1, if\ Z < 0 \end{cases}.$$

From equation (6), $\tilde{Z}_{n+1}$ is the equation which has been added into the map $\emptyset$ defined in equation (4). One can see that $\tilde{Z}_{n+1}$ is an equation that depends on X_n, Y_n, X_{n+1}, and Y_{n+1}.

The behavior of the orbit of $\widetilde{\Phi}$ happens to be periodic for some values of initial conditions. By choosing a specific initial condition and values of parameter α and β, the orbit of $\widetilde{\Phi}$ defined in equation (6) rotates around its center point and closes its orbit (return to its original initial condition) $\bar{\alpha} = \frac{\alpha}{gcd(\alpha,2\beta)}$ times.

Numerical Experiments on Case II

For this Case II, it turns out that the orbit of $\widetilde{\Phi}$ is also periodic with period $\bar{\alpha}$ for some values of initial conditions (x_0, y_0, z_0) in the 3-D discrete space which will be discussed later in the next section. In this Case II, the behavior of the orbit of $\widetilde{\Phi}$ is more complicated as compared to the orbit of $\overline{\Phi}$ in Case I. One observes that the elliptic-type orbits of the map $\widetilde{\Phi}$ formed a "twisted" version (see Figure 5) of the map $\overline{\Phi}$ and of the original discrete map $\emptyset$ explained in Figure 3. Moreover, the elliptic-type orbits are no longer formed as shown in Figure 5 below.

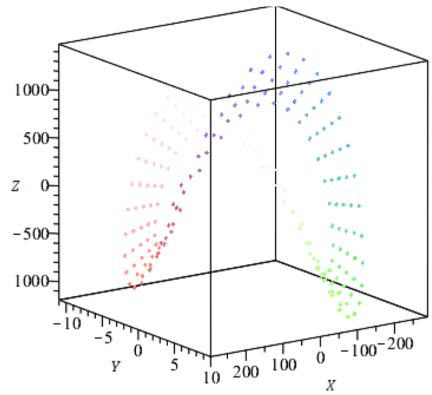

(a)

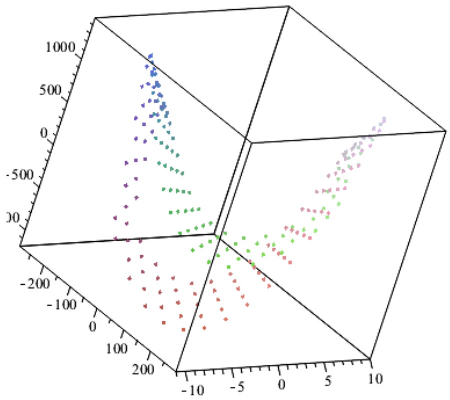

(b)

Figure 5: The orbit of $\widetilde{\Phi}$ defined in equation (6) with $\alpha = 5, \beta = 2$.

In Figure 5, one can see that the orbit of $\widetilde{\Phi}$ f has no longer preserve the elliptic-type orbits form but instead, forms similar to a discrete version of the hyperbolic paraboloid equation or as known as the "potato chip' equation (see Figure 6(b)), generated by,

$$f(x, y) = \frac{y^2}{b^2} - \frac{x^2}{a^2}. \tag{7}$$

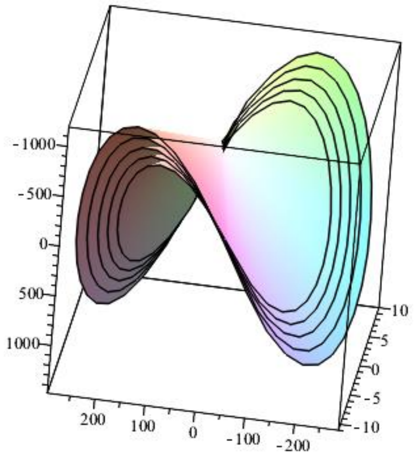

(a)

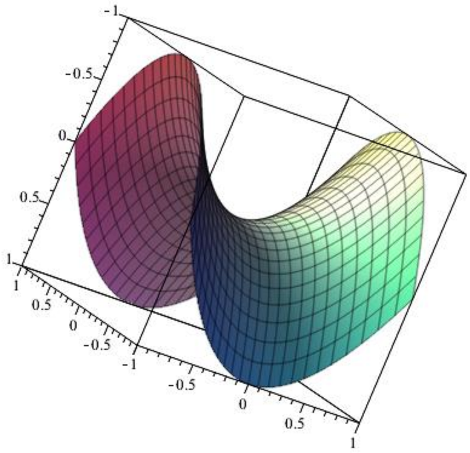

(b)

Figure 6: a) The orbit of $\widetilde{\Phi}$ (in $\mathbb{Z}^{\mathbf{3}}$) defined in equation (6) in a polygon plot in Maple Software. b) The figure of hyperbolic paraboloid equation defined in equation (7) in Maple Software.

In Figure 6, it can be observed that the map of $\widetilde{\Phi}$ is different than the map of hyperbolic paraboloid defined in equation (7). Furthermore, the phase space of the orbit of $\widetilde{\Phi}$ is also different (in $\mathbb{Z}^3$) than the phase space of the hyperbolic paraboloid viewed in $\mathbb{R}^3$. In the Figure 6(a), the orbit points are bounded by the "most" outer orbits point of the map $\widetilde{\Phi}$ and these orbit points are periodic with period of $\bar{\alpha} = \frac{\alpha}{gcd(\alpha,2\beta)}$. In Figure 6(b), the orbits of the map bounded on the surface with no restriction with respect to the *Z*-axis.

Results and Discussion

As described in the previous discussion of the map of $\overline{\Phi}$ defined in equation (5) for Case I, the original XY-plane is lifted by a 45° angle from the horizontal plane (see Figure 7). Thus, we have the following.

Lemma 1 *Let $\mathbb{Z}_+$ be the set of non-negative integers and let (y_n, z_n) (and (y_k, z_k) be two points in the orbit of $\overline{\Phi}$ map defined in (5) on the $YZ-plane$ where $n, k \in \mathbb{Z}_+$. Thus, from the projection on the $X-axis$, the angle of the YZ-plane from the orientation of the X-axis the is given by*

$$\tan\theta = \frac{|Z_n - Z_k|}{|Y_n - Y_k|} = 1, \tag{8}$$

where $\theta = 45°$.

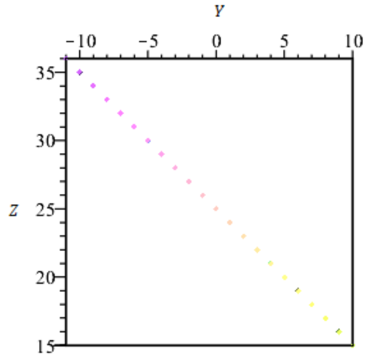

(a)

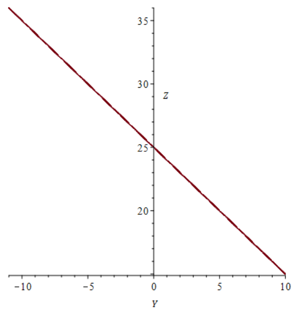

(b)

Figure 7: a) The orientation of X (side view from X) on the YZ-plane. B) The 2-D map of $\overline{\Phi}$ on the YZ-plane.

The Figure 7 shows that the angle θ, of the YZ-plane from the X-axis is 45°. From the numerical experiments, on the YZ-plane, the orbit of $\overline{\Phi}$ defined in equation (5) rotates around its center point (not necessarily the origin (0,0,0)) $\bar{\alpha} = \frac{\alpha}{gcd(\alpha,2\beta)}$ times (see Figure 4). Hence, we have the following:

Conjecture 2 (Case I) *Let* $\bar{\alpha} = \frac{\alpha}{gcd(\alpha,2\beta)}$ *and let* $\overline{\Phi}$ *is the 3-dimensional map defined in* equation *(5). Then, for any sufficiently large initial conditions* (x_0, y_0, z_0), *all orbits of* $\overline{\Phi}$ *are periodic with period* $\bar{\alpha}$ *in the 3-dimensional lattice.*

Here, the sufficiently large initial conditions refer to the values of (x_0, y_0, z_0) which is far away from the center point.

Now, let us describe the geometric interpretation of the map $\overline{\Phi}$ defined in equation (5) or Case I (Dawkins, n.d.). The 3-D map equation is determined by relating the points on the plane with its orientation. This orientation is specified by finding the normal vector to the map. Generating two vectors from the chosen three points, vector multiplication is performed between the generated vectors to produce a vector that is normal to the map.

The standard equation of the plane is then derived in terms of the vector normal as $\vec{n} \cdot \overrightarrow{P_0P} = 0$, where the first vector is the normal vector, and the second vector is related to arbitrary point $P(x,\ y,\ z)$ on the plane with respect to one point on the map.

For Case I, with the values of parameter $\alpha = 5$ and $\beta = 2$, the equation of the 3-D map is then simplified as the equation of 2-D plane in space as $y + z - 70 = 0$.

Equivalently, this equation represents the equation of straight line in the YZ-plane as shown in Figure 6. The line has a negative slope equivalent to 45° with respect to the Y-axis which satisfies the Lemma 1 (equation (8)). To satisfy the conditions in Case I, the variable x should satisfy the equation (5). Depending on the values of α and β, the equation of the 2-D plane changes. However, it is observed that for any values of α and β, there is no vector x that is $\langle 0, y, z\rangle$.

For Case II as described in previous section, the map $\widetilde{\Phi}$ becomes periodic with period $\bar{\alpha} = \frac{\alpha}{gcd(\alpha,2\beta)}$. We have the following:

Conjecture 2 (Case II) *Let* $\bar{\alpha} = \frac{\alpha}{gcd(\alpha,2\beta)}$ *and let* $\widetilde{\Phi}$ *be the 3-Dimensional map defined in* equation *(6). Then for some initial conditions* (x_0, y_0, z_0), *the orbit of* $\widetilde{\Phi}$ *defined in* equation *(6) is periodic with period* $\bar{\alpha}$ *in the 3-dimensional lattice.*

As mentioned in the previous section, the behavior of the orbit in Case II is complicated as compared to Case I. This is because one needs to choose a specific value of initial condition (x_0, y_0, z_0) that has the period of the orbit of $\widetilde{\Phi}$ is periodic with period $\bar{\alpha}$.

It happens that if we choose an initial condition (specifically a point after one iteration of the chosen initial point in its own orbit), the orbit of the 3-D map defined in Case II is periodic with period $\bar{\alpha}$. However, it does not happen if we choose arbitrary initial conditions. In this Case II, the orbit of the 3-D map defined in equation (6) can be non-periodic for arbitrary initial conditions.

Conclusion

It is shown that by adding and varying the Z-axis in the 2-Dimensional original map to the 3-Dimensional map, the periodicity may be attained under a certain Z-axis conditions. If we tilt and lift the XY-plane, we can see that it is still periodic for sufficiently large initial conditions (Case I). In another situation, we can still sustain its periodicity by twisting the plane like in the Case II (for some initial conditions (x_0, y_0, z_0)). In this project, this 3-D lattice is a wide space where the form of the 2-D elliptic-type orbits may and may not cover the whole 3-D space. In fact, its 2-D form of the discrete Chirikov-Taylor standard map can be viewed in the 3-D space depending on the Z-axis defined in Case I and II.

However, we were unable to accomplish periodicity in the more complicated versions of Z-axis or in the 3-D space. Thus, we classified them as non-periodic cases even though the orbit of the map defined in equation (4) which has period $\bar{\alpha}$ is originally periodic case in 2-D. This is because of the infinite number of types of functions for the Z-axis which can be defined or added (not necessarily for Case I and Case II only) in the 2-D map in equation (4). Since we only focus on the orbit of the 3-D maps which give periodicity, therefore we only obtained two types of functions of Z that preserve the rotations as defined in equations (5) and (6).

For future, further investigation could be explored related to the statistical properties of 3-D representation especially in describing the behaviour of the discrete points in a specific lattice. This study is useful in viewing the 3-D map which was constructed from the 2-D problem and could give new interpretation from the statistical point of view.

Acknowledgement

This research was financially supported by the International Islamic University Malaysia (IIUM) Research Management Centre Grant (RMCG) under project RMCG20-005-0005.

References

Chirikov B. V., Izrailev F. M., & Shepelyansky D. L. (1981). Dynamical stochasticity in classical and quantum mechanics. *Soviet Scientific Reviews Section C, 2*, pp. 209.

Chirikov, B.V. (1983). Chaotic Dynamics in Hamiltonian Systems with Divided Phase Space. In: L. Garrido (Ed.) *Dynamical System and Chaos. Lecture Notes in Physics, 179*. Springer, Berlin, Heidelberg.

Chirikov, B. V., & Shepelyansky, D. L. (1984). Correlation Properties of Dynamical Chaos in Hamiltonian Systems. *Physica 13D*.

Chirikov, B. V. (1969). *Research Concerning The Theory of Nonlinear Resonance and Stochasticity*, CERN Libraries, Geneva.

Chirikov, B. V. (1979). A Universal Instability of Many-dimensional Oscillator Systems. *Physics Reports 52*(5), 263-379.

Vivaldi, F., & Bailin, H. (2016). Discrete Resonances. In: K. P. Kok & G. Molin (Eds.) *Peregrinations from Physics to Phylogeny*. World Scientific.

Rannou, F. (1974). Numerical studies of discrete plane area-preserving mappings. *Astronomy and Astrophysics 31*, 289–301.

Zhang, X. S., & Vivaldi, F. (1998). Small perturbations of a discrete twist map. *Annales de l'IHP Physique théorique, 68*(4), 507-523.

Finn, C. (2012). *Chaotic Control Theory Applied to the Chirikov Standard Map*. BSc thesis, University College Dublin.

Jürgen, P. (2001). A Lecture on The Classical KAM Theorem. In: A. Katok, R. Llave, Y. Pesin, & H. Weiss (Eds.) *Smooth Ergodic Theory and Its Applications, Proceedings of Symposia in Pure Mathematics, 69* (pp 707-732). American Mathematical Society, Rhode Island.

Alwani, F., & Vivaldi, F. (2018). Nonlinear rotations on a lattice. *Journal of Difference Equations and Applications, 24*(7), 1074-1104.

Heinrich, M. P., & Hansen, L. (2020). Highly Accurate and Memory Efficient Unsupervised Learning-Based Discrete CT Registration Using 2.5D Displacement Search. *Proceedings of the 23rd In International Conference on Medical Image Computing and Computer-Assisted Intervention (MICCAI 2020), Lima, Peru, 4-8 October 2020*, 190-200.

Samaniego, F., Sanchis, J., García-Nieto, S., & Simarro, R. (2017). UAV motion planning and obstacle avoidance based on adaptive 3D cell decomposition: Continuous space vs discrete space. *Proceedings of the Second Ecuador Technical Chapters Meeting (IEEE), Ecuador, 16-20 October 2017*.

Hofmann, F., Tarleton, E., Harder, R. J., Phillips, N. W., Ma, P. W., Clark, J. N., Robinson, I. K., Abbey, B., Liu, W., & Beck, C. E. (2017). 3D lattice distortions and defect structures in ion-implanted nano-crystals. *Scientific reports, 7*(45993).

Thibault Y. (2010). *Rotations in 2D and 3D Discrete Spaces* [Doctoral dissertation, Université Paris-Est, France].

Dawkins, P. *Calculus III*. Retrieved January 10, 2023, from http://tutorial.math.lamar.edu.

Haramburu, P. (2006). Exploring Non-linear 3D dynamical Systems. *Proceedings of the 2006 International Conference on Modeling, Simulation & Visualization Methods, Las Vegas, Nevada, USA, 26-29 June 2006*.

Lucas S, Sander E., & Taalman L. (2020). Modeling Dynamical Systems for 3D Printing. *Notices of the American Mathematical Society, 67*(11), 1692-1905.

Bane A. (2012) *3D Animation Essentials.* Indianapolis, Indiana: John Wiley & Sons.

Article History
Received: 01/09/2023
Accepted: 01/12/2023